

The Mini Wheelbot: A Testbed for Learning-based Balancing, Flips, and Articulated Driving

Henrik Hose, Jan Weisgerber, and Sebastian Trimpe

Abstract—The Mini Wheelbot is a balancing, reaction wheel unicycle robot designed as a testbed for learning-based control. It is an unstable system with highly nonlinear yaw dynamics, non-holonomic driving, and discrete contact switches in a small, powerful, and rugged form factor. The Mini Wheelbot can use its wheels to stand up from any initial orientation – enabling automatic environment resets in repetitive experiments and even challenging half flips. We illustrate the effectiveness of the Mini Wheelbot as a testbed by implementing two popular learning-based control algorithms. First, we showcase Bayesian optimization for tuning the balancing controller. Second, we use imitation learning from an expert nonlinear MPC that uses gyroscopic effects to reorient the robot and can track higher-level velocity and orientation commands. The latter allows the robot to drive around based on user commands – for the first time in this class of robots. The Mini Wheelbot is not only compelling for testing learning-based control algorithms, but it is also just fun to work with, as demonstrated in the video of our experiments at https://youtu.be/_d7AqTRjz6g.

I. INTRODUCTION

Experimental validation is an integral part of robotics research that even grows in importance with data-driven and learning-based control relying on real-world data. To test novel algorithms, researchers have proposed a multitude of balancing and driving robots in recent years [1]–[5]. However, driving robots lack the challenge of instability, and pure balancing lacks mobility and thus higher-level tasks, as we will detail in the discussion of related work. Despite many practical robots having nonlinear, unstable, and hybrid system behavior (e.g., quadcopters [6] and legged robots [7]), small-scale test systems with all these properties are rare. We think that validating learning algorithms in the presence of uncertainty requires i) safety, ii) robustness (i.e., not break easily), and iii) automatic experimentation (i.e., reset after failure), all of which we aim to achieve.

The Mini Wheelbot is a symmetric, reaction wheel, balancing unicycle robot with directly controlled, unstable roll and pitch dynamics. The yaw state is uncontrollable for the linearized system. This necessitates nonlinear methods utilizing gyroscopic effects to achieve articulated (meaningful) driving. The ability to stand up from any initial position enables environment resets for automated experiments. Additionally, the Mini Wheelbot is powerful enough for interesting maneuvers like flips. These episodic and continuing tasks are abstractions of typical learning problems in robotics. In

This work is funded in part by the German Research Foundation (DFG) – RTG 2236/2 (UnRAVeL). Simulations were performed with computing resources granted by RWTH Aachen University under project RWTH1621.

All authors are with the Institute for Data Science in Mechanical Engineering (DSME), RWTH Aachen University, Germany, {henrik.hose, trimpe}@dsme.rwth-aachen.de

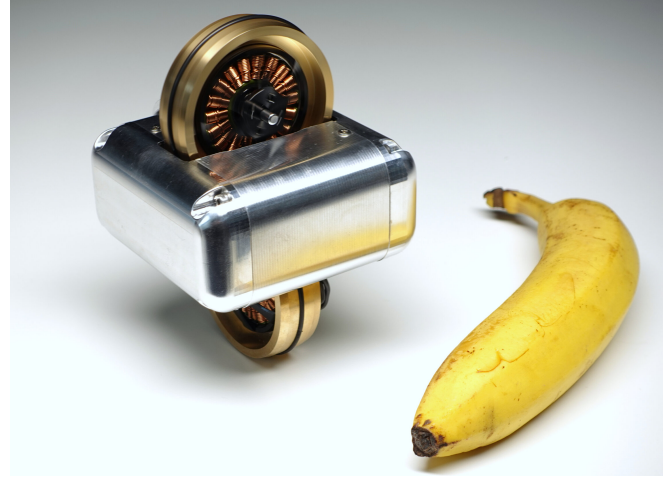


Fig. 1: The Mini Wheelbot: A small, rugged, and symmetric reaction wheel unicycle robot with challenging nonlinear, unstable, and hybrid dynamics. The Mini Wheelbot can stand up from any position which allows for automatic environment resets in learning-based control experiments.

this paper, we showcase two learning-based algorithms to solve them. First, we use Bayesian optimization (BO) to tune a balancing controller with minimal human intervention due to automatic resets. Second, we approximate a sophisticated model-predictive controller (MPC) with a fast-to-evaluate neural network to control the yaw orientation and drive around based on keyboard commands.

The Mini Wheelbot is a complete re-design that substantially advances an early prototype in [1]: It is smaller, more robust, and has a powerful CPU running Linux while being affordable with bill of material costs of \$1200 per robot (at quantity ten). In summary, we make the following contributions:

- 1) The Mini Wheelbot, a small, powerful, rugged, open-source robot ideal for learning-based control experiments due to automatic environment resets and interesting dynamics.
- 2) Implementation of two state-of-the-art learning approaches (BO for controller tuning, approximate MPC) to illustrate the versatility as a learning testbed.
- 3) With the approximate MPC, we achieve yaw control and thus articulated (meaningful) driving for the first time for this type of robot.

A video of the Mini Wheelbot and our experiments is available at https://youtu.be/_d7AqTRjz6g.

II. RELATED WORK

Small-scale driving [3]–[5], [8]–[18] and balancing [1], [2], [19]–[23] robots are a popular choice for control experiments, though none is specifically designed for testing learning algorithms. This section summarizes existing designs, highlighting that either articulated driving or balancing of an unstable system is achieved. In contrast, the Mini Wheelbot combines both with highly nonlinear yaw dynamics and automatic environment resets ideal for learning experiments.

A. Driving Robots

Driving robots have been developed for decades, commonly with slow and stable differential drives [8]–[14] or fast and car-like dynamics for autonomous racing [3]–[5], [15]–[18]. Differential-drive platforms are cheap to produce in large quantities for testing networked and multi-robot control algorithms [9], [12]–[14], [24], [25], or as education systems [8], [10], [11]. Research questions arise mainly from high-level perception and coordination while simple kinematic planning and state-feedback controllers perform well in steering. On car-like robots, pushing the limits of autonomous racing requires precise control of fast dynamics and difficult-to-model tire slip effects, however, the underlying contouring control problem can be linearized and is inherently stable when driving slowly, hence even PID schemes succeed in this task [3]. In comparison, the Mini Wheelbot is unstable and has interesting nonlinear tasks (yaw control) that can not be achieved by classic linear methods.

B. Balancing Robots

Balancing is a long-standing challenge in robotic research, for example in pendulum sculptures [2], [19], [20], [26], unicycle robots [1], [27]–[37] like the Mini Wheelbot, and even legged [22] or ball [23] robots. Cube-like robots stabilize standing on a corner with leavers [26] or reaction wheels [2], [19], [20], where nonlinearity [21] and underactuation [2] inspire research. While some cube-like robots can automatically stand up [19]–[21], their mobility is restricted to walking-like sequences of controlled stand-up and falling. Similarly, the Mini Wheelbot can use its reaction wheel to balance on the point contact of the driving wheel, stand up from any initial position, and has underactuated yaw dynamics. That is, when in perfect balance, the Mini Wheelbot has no direct control over its yaw angle. Compared to cube-like robots, however, the driving wheel allows for mobility.

Balancing unicycle robots use levers [27], [29], [30], [37] or reaction wheels [1], [31], [32], [34]–[36]. Except for an early prototype [1], existing designs’ actuators lack power for a stand-up and are asymmetric, which prohibits interesting chaining of stand-up maneuvers. Roll and pitch balancing with linear state-feedback or fuzzy controllers is well understood [29], [31], [32], [35], also with reference velocities [34]. However, so far, a third turntable actuator was required to control the yaw orientation [27], [28], [36], [37] and thus permit meaningful driving. In contrast, we use nonlinear methods to control yaw without an additional turntable actuator for the first time.

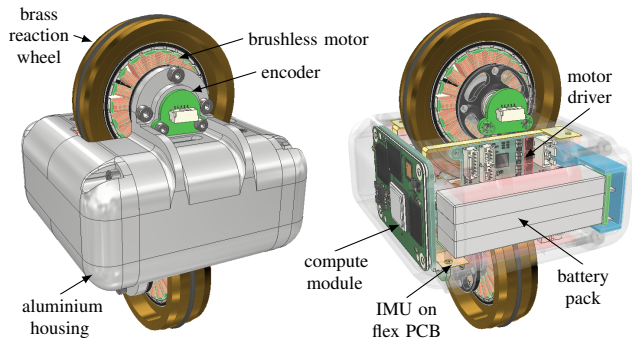


Fig. 2: System overview of the Mini Wheelbot.

III. DESIGN OF THE MINI WHEELBOT

The Mini Wheelbot needs to be small, rigid, and powerful for learning experiments. In this section, we summarize the custom design of hardware and electronics that is necessary to achieve these design goals and meet the specifications listed in Tab. I.

TABLE I: Specifications of the Mini Wheelbot.

Spec.	Value
Dims.	130 mm (height) x 87 mm (width)
Weight	Total 0.69 kg, wheels 0.13 kg (each), body 0.43 kg
Motors	T-Motor MN4006, max. 8000 rpm, 0.5 N m
Battery	450 mAh, 22.2 V, 6S LiPo, max. cont. 20 A discharge
Runtime	45 min when balancing
CPU	Pi CM4, BCM2711 quad-core Cortex-A72, 1.5 GHz
Sensors	4x Bosch BMI088 IMU, 2x AMS AS5047D 14bit encoder
System	RT-Preempt Linux, Buildroot

A. Mechanical Design

The Mini Wheelbot is designed to be compact, rugged, and powerful. Its size is determined by the onboard compute module (a Raspberry Pi CM4) and six battery cells. Brass is chosen as material for the reaction wheels due to its high density and good availability at CNC job shops. Sizing calculations of the reaction wheels were performed as described in [1] to maximize rotational inertia needed for the stand-up maneuvers. The body is made from aluminum, which is lightweight, durable, and inexpensive to machine. Inside the body, compute module, battery pack, and power electronics are packed tightly (see Fig. 2). The packaging minimizes body mass and inertia for highly dynamic maneuvers like stand-up and flips while keeping symmetry.

B. Electronics Design

The custom electronics inside the Mini Wheelbot are designed to maximize the robots power and control performance while ensuring safety and battery runtime. An overview of custom electronics is shown in Fig. 3. Schematics for all components are available online¹.

The removable battery pack has six 450mAh Lithium Polymer cells (three on each side of the robot) protected by

¹<https://github.com/wheelbot/mini-wheelbot>

two BQ77915 with overcurrent and short-circuit protection – all safely potted in one housing (Fig. 3, bottom left). The power distribution board monitors power consumption and engages a braking resistor in case recuperated current during stand-up maneuvers can not be charged back into battery or external power supply. In addition, a nRF24L01P communicates with a wireless emergency stop button to shut off motor controllers. Two custom inverters based on the μ Motor [38] run field-oriented control (FOC) to drive T-Motor MN4006 brushless DC motors. Current is measured low-side on all phases at FOC loop frequency of 40 kHz. Due to careful analog design and INA21A2 current sense amplifiers, the gains of the PI d-q-current controllers can be chosen as high as 10 kHz bandwidth. On-axis magnetic 14-bit AS5047 encoders are interfaced by the inverters via SPI with transfers triggered from an interrupt synchronized with the FOC loop. The motors exhibit strong cogging with peaks of up to 20 mNm (4% of the maximum torque). This severely impacts balancing control. We therefore implement cogging compensation with a lookup table of feedforward torques. These are calibrated by sweeping through a full rotation in 4000 steps with a high-gain position controller and saving the average current to hold each position in flash memory on the inverter (cf. [39] for details). The compensation effectively reduces the cogging to less than 2.5 mNm (0.5%). Power distribution and inverters are commanded via CAN-FD with an MCP2517FD controller by the Raspberry Pi CM4 compute module at 1 kHz. Bosch BMI088 IMUs are directly interfaced via I2C from the CM4.

C. Software

The Mini Wheelbot runs a Buildroot Linux with real-time kernel. The single-board computer performs all higher-level estimation and control, implemented in C++ and running inside a Docker container. While sending CAN messages through Linux SocketCAN is almost latency free in this setup, there is significant delay (up to 10 ms) between the kernel interrupt and receiving encoder values on the user-space socket. This delay is due to the processing of received CAN messages by the same workers as all other networking and can be compensated in software by extrapolation. IMUs readings are available through the Linux IIO subsystem.

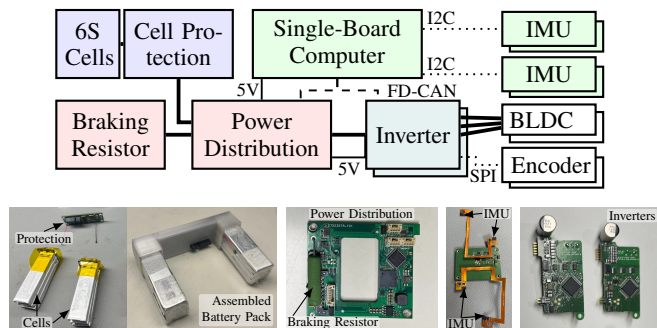


Fig. 3: Electronics design of the Mini Wheelbot (top) and custom circuit boards (bottom).

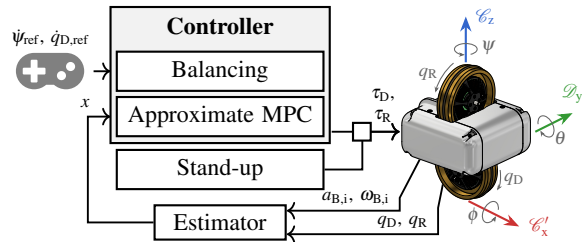


Fig. 4: Control system overview and generalized coordinates.

IV. A VERSATILE CONTROL TESTBED

This section details the control methods on the Mini Wheelbot, as visualized in Fig. 4, that we later use in illustrative learning tasks in Sec. V. To this end, we first describe the system model (Sec. IV-A) and optimization-based identification of parameters from trajectory data (Sec. IV-B), before introducing the state-feedback controller used for balancing (Sec. IV-C), and a nonlinear model-predictive controller for the orientation of the robot that is required for meaningful driving (Sec. IV-D). Finally, the stand-up in the roll and pitch direction and a half-flip are described (Sec. IV-E and IV-F). All implementations are available online¹.

We omit a detailed description on the estimation of the robots state, as we implement the existing method from [1] to fuse four gyroscope² $\omega_{B,i}$, four accelerometer $a_{B,i}$, and two wheel encoder $q_{D,R}$ measurements (cf. [19], [21], [26], [40] for details). Notably, the presented controllers are robust to alignment errors of the IMUs thus no calibration is needed.

A. System Model

The Mini Wheelbot's state can be described as $x = [\psi, \phi, \theta, \dot{\psi}, \dot{\phi}, \dot{\theta}, q_D, q_R, \dot{q}_D, \dot{q}_R]^T$. The body orientation is expressed in Euler-like angles in yaw-roll-pitch order (see Fig. 4) with yaw ψ and roll ϕ around the contact point coordinate system's \mathcal{C}_z axis and resulting \mathcal{C}'_x axis, and pitch θ around the drive motors axis of rotation that is aligned with \mathcal{D}_y . The angles of the wheels are $q_{D,R}$ and the actions $u = [\tau_D, \tau_R]^T$ are the torques applied to driving (bottom) and the reaction (top) wheel. The Mini Wheelbot's nonlinear, continuous-time dynamics of implicit form $f_{ct}(x, \dot{x}, u, p) = 0$ with parameters p can be derived using standard, multi-body methods (e.g., Euler-Lagrange equations). A detailed symbolic derivation using a computer algebra system is given in the supplementary code¹ and described in detail in [30]. The resulting differential equations have the form:

$$M(\phi, \theta, p)[\ddot{\phi}, \ddot{\theta}, \ddot{\psi}, \ddot{q}_D, \ddot{q}_R]^T + b(\phi, \theta, \psi, \dot{\phi}, \dot{\theta}, \dot{q}_D, \dot{q}_R, p) + g(\phi, \theta, \tau_D, \tau_R, p) + \tau_\psi(\psi, p) = 0. \quad (1)$$

The implicit dynamics (1) are parameterized by $p = [m_{D,R}, m_B, I_{D_{x,z}, R_{y,z}}, I_{D_{y,R}, x}, I_B, r_{D,R}, l_{D,R}, C_1, C_2] \in \mathbb{R}^{11}$, which consists of the masses and mass moments of inertia

²Using corrected gyroscope measurement equations from the errata of [1].

of the robot's body m_B and I_B and reaction wheels $m_{D,R}$ and $I_{D,R}$. The mass moments of inertia are assumed to be diagonal and share values for multiple axis due to (quasi-)symmetries. Further, the radius of the wheels $r_{D,R}$ and distance between rotation axis $l_{D,R}$ enter as geometric parameters. The rotational friction in the contact point is modeled as $\tau_\psi = C_1 \tanh(C_2 \psi)$, where the constant C_1 models the magnitude and C_2 the slope of the friction. The mass matrix $M(\phi, \theta)$ is difficult to invert symbolically (i.e., symbolically computing $\dot{x} = f_{\text{expl}}(x, u, p)$) and (1) is stiff on a timescale relevant for controlling the yaw orientation. Both issues motivate the use of implicit integrators [41] for an accurate discrete-time model with time $t \in \mathbb{N}$, that is:

$$x(t+1) = f_{\text{dt}}(x(t), u(t), p). \quad (2)$$

B. Optimization-based Parameter Identification

In this section, the optimization-based identification of the parameters p from data is described, which is similar to the methods presented in [4], [42]–[44]. To this end, an optimization problem

$$\begin{aligned} \min_{p \in \mathcal{P}, \hat{x}, \hat{u}} & \sum_{i=0}^{N_{\text{id}}} \sum_{t=0}^{T_{\text{id}}} \|\hat{x}_i(t) - \bar{x}_i(t)\|_{Q_{\text{id}}}^2 + \|\hat{u}_i(t) - \bar{u}_i(t)\|_{R_{\text{id}}}^2 \\ \text{s.t.} & \hat{u}_i(t) - \bar{u}_i(t) \in \mathcal{W}, \forall t \in \mathbb{I}_{T_{\text{id}}}, \forall i \in \mathbb{I}_{N_{\text{id}}} \\ & \hat{x}_i(t+1) = f_{\text{dt}}(\hat{x}_i(t), \hat{u}_i(t), p) \forall t \in \mathbb{I}_{T_{\text{id}}}, \forall i \in \mathbb{I}_{N_{\text{id}}} \end{aligned} \quad (3)$$

is solved, where the parameters are constrained to reasonable box constraints \mathcal{P} , the optimization objective consists of quadratic cost on the error between predicted \hat{x} and measured state \bar{x} and predicted \hat{u} and measured action \bar{u} over a finite horizon T_{id} and a set of trajectories N_{id} . The input disturbance constraint set \mathcal{W} can be conservatively approximated from direct measurements of the actuator torque ripple. Quadratic cost matrices are chosen empirically as diagonal matrices $Q_{\text{id}} = \text{diag}([100, 1, 1, 10, 10, 10, 0.1, 0.1, 0.1, 0.1]^\top)$ and $R_{\text{id}} = \text{diag}([100, 100]^\top)$.

The optimization problem (3) is implemented in CasADi [45] and solved with IPOPT [46], which yields the optimal parameters p^* . A selection of trajectories from the dataset and the achieved prediction for the critical yaw state is plotted in Fig. 5. In the following, the discrete-time dynamics (2) with p^* substituted in will be referred to as $f_{\text{dt}}(x(t), u(t))$, dropping the explicit dependency on p for ease of notation.

C. Balancing State-Feedback Controller

The Mini Wheelbot can balance in the roll and pitch direction using a simple state-feedback controller as proposed in [1]. While we use the same structure, that is, state-feedback for the roll and the pitch states separately, we choose a data-driven approach to tune the gains of the controllers directly from closed-loop experiments instead of LQR (see Sec. V-A).

The state feedback controller $u(t) = Kx(t)$ has the feedback gains matrix

$$K = \begin{bmatrix} 0 & 0 & K_{D1} & 0 & 0 & K_{D2} & K_{D3} & 0 & K_{D4} & 0 \\ 0 & K_{R1} & 0 & 0 & K_{R2} & 0 & 0 & K_{R3} & 0 & K_{R4} \end{bmatrix}, \quad (4)$$

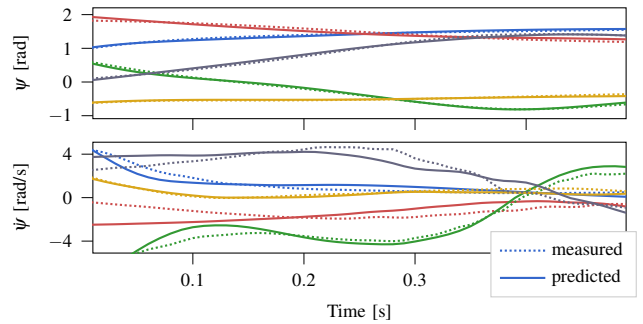


Fig. 5: Five of the trajectories used for parameter identification: measurements (dotted) of yaw angle (top) and yaw rotational velocity (bottom) and predictions with optimal parameters p^* (solid).

where the gains $K_D \in \mathbb{R}^4$ control pitch and $K_R \in \mathbb{R}^4$ roll.

Remark: The yaw orientation of the robot is non-controllable for the Mini Wheelbot's dynamics linearized about the equilibrium balancing position, which are $A = \frac{\partial f_{\text{expl}}}{\partial x}|_{x=0, u=0}$ and $B = \frac{\partial f_{\text{expl}}}{\partial u}|_{x=0, u=0}$. The controllability matrix $C = [B, AB, A^2B, \dots]$ has $\text{rank}(C) = 9 < 10$ where the non-controllable state is ψ . Yet, friction in the wheel-to-ground contact lets ψ converge to standstill.

D. Nonlinear MPC for Driving Control

Controlling the Mini Wheelbot's yaw orientation is required for driving the robot along meaningful paths, but can not be achieved by simple, linear control methods. We propose using a nonlinear MPC [47] for controlling the yaw orientation. In MPC, an optimization problem is repeatedly solved to compute a sequence of optimal actions that minimize a cost function for predicted future states. From the sequence of optimal actions, only the first is applied in closed loop before solving the optimization problem again. For the Mini Wheelbot, we formulate the nonlinear MPC

$$\min_{v, x} \sum_{k=0}^{N_{\text{MPC}}} \|x(t|k)\|_{Q_{\text{MPC}}}^2 + \|u(t|k)\|_{R_{\text{MPC}}}^2 \quad (5a)$$

$$\text{s.t. } x(t|k+1) = f_{\text{dt}}(x(t|k), u(t|k)), \quad (5b)$$

$$u(t|k) = Kx(t|k) + v(t|k), \quad (5c)$$

$$x(t|k) \in \mathcal{X}, u(t|k) \in \mathcal{U} \forall k \in \mathbb{I}_{N_{\text{MPC}}-1} \quad (5d)$$

$$x(t|0) = x(t), \quad x(t|N_{\text{MPC}}) \in \mathcal{X}_f \quad (5e)$$

that includes pre-stabilizing feedback (5c) with the controller from Sec. IV-C and a terminal constraint (5e). The terminal constraint is $\mathcal{X}_f = 0$ to guarantee convergence of the solver to a solution that drives the yaw angle to the desired setpoint. After solving the optimization problem (5), the first action is applied to the system, $u(t) = u^*(t|0)$. Cost terms are empirically chosen as diagonal matrices $R_{\text{MPC}} = \text{diag}([10, 0.01]^\top)$ and $Q_{\text{MPC}} = \text{diag}([100, 1, 1, 0.001, 0.01, 1, 1, 0.0001, 0.25, 0.001]^\top)$.

Details on the constraints are available in the supplementary code¹. We implement the nonlinear MPC optimization problem (5) in CasADi [45] and solve it with IPOPT [46].

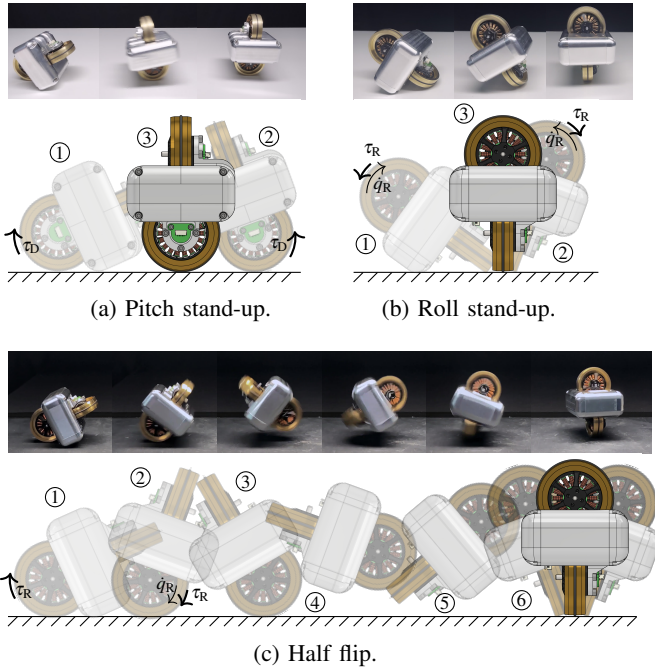


Fig. 6: Environment reset and half flip: The Wheelbot can stand up from any side by using its driving wheel (top left), its reaction wheel (top right), and even perform a flip stand-up (bottom). The maneuvers can be chained to reliably perform environment resets in episodic tasks.

E. Stand-Up Maneuver

Similar to [1], the new Mini Wheelbot can stand up in the pitch and roll direction (see Fig. 6a and 6b). Standing up in the pitch direction involves one wheel quickly driving under the robot. For the roll stand-up, the robot first spins up the reaction wheel before rapidly decelerating it thus exerting a counter torque that makes the robot stand up. Both maneuvers are achieved via precomputed, open-loop command sequences before switching on the state-feedback controller (see Sec. IV-C) when entering $\pm 30^\circ$ roll and pitch.

F. Half Flip

We implement a novel half-flip stand-up maneuver, visualized in Fig. 6c. This acrobatic maneuver pushes the Mini Wheelbot to its limits, illustrating the power of the hardware and hinting at future complex high-speed learning tasks. The half flip is executed from an open loop action sequence taking about 160 ms before switching on the balancing state-feedback controller for landing. Similar to the pitch stand-up maneuver, the drive wheel quickly drives under the robot, however, with much higher torque, thus accelerating the Mini Wheelbot beyond the upright position. After a 180° rotation, the balancing position on the other wheel is reached, where the state-feedback controller starts balancing.

V. LEARNING-BASED CONTROL EXPERIMENTS

The Mini Wheelbot involves a number of challenges, making it an interesting testbed for data-driven, learning-based control algorithms. We showcase two of such algorithms.

In Sec. V-A, we use BO which has become popular for controller tuning in the last decade [48]–[52] and allows us to automatically find excellent balancing controller gains in automated hardware experiments. In Sec. V-B, we use imitation learning from an expert MPC, also called approximate MPC (see [53] for a recent survey). Approximate MPC avoids slow online optimization which enables sophisticated nonlinear MPC in fast feedback loops onboard robots [54], [55] even on low-cost hardware [56].

A. Tuning Stand-up & Balancing via Bayesian Optimization

BO describes a family of black-box optimization algorithms that can be used for controller tuning based on a few interactions with the real world system [48]–[52]. Instead of LQR in [1], we use BO to tune the gains of the state-feedback controller (4) in a direct, data-driven approach based on rewards collected in real-world experiments. This is practically motivated: Tuning LQR cost matrices can be unintuitive and for some gain combinations, unmodeled high-frequency oscillations occur that are difficult to avoid through the choice of LQR cost. In addition to finding excellent balancing controller gains, BO illustrates the advantage of automatic environment resets through the Mini Wheelbot’s stand-up maneuvers for learning on episodic tasks.

With BO, we find

$$K^* = \arg \max_K V(K) \quad (6)$$

based on (noisy) real-world evaluations of the true objective function $V(K)$. We define the objective function to be

$$V(K) = \begin{cases} -J_c, & \text{if crash,} \\ -\frac{1}{T_{\text{BO}}} \sum_{t=0}^{T_{\text{BO}}} \|x(t)\|_{Q_{\text{BO}}}^2 - w_{\text{vib}} \cdot J_{\text{vib}}, & \text{else,} \end{cases} \quad (7)$$

where T_{BO} is the experiments time horizon. The crash penalty J_c is empirically chosen slightly worse than a barely successful experiment (e.g., $J_c = 30$ for the experiment shown in Fig. 8). For successful experiments, the objective value consists of the mean squared error over the state deviation from the equilibrium with diagonal weights $Q_{\text{BO}} = \text{diag}([0, 50, 200, 0, 0.4, 0.1, 0, \dots]^T)$. The additional penalty J_{vib} weighted by $w_{\text{vib}} = 10^{-5}$ is

$$J_{\text{vib}} = \sum_{t=1}^{T_{\text{BO}}} (|\Delta \dot{\phi}(t)|, \text{if } |\Delta \dot{\phi}(t)| \geq \alpha, \text{ else } 0), \quad (8)$$

with $\Delta \dot{\phi}(t) = \dot{\phi}(t) - \dot{\phi}(t-1)$, which effectively suppresses high frequency vibrations.

For each episode of the optimization, the Wheelbot has to perform a stand-up maneuver and balance with a setpoint change in the drive-wheel position. An excerpt of the closed loop trajectories from our experiments when the controller stabilizes the robot right after the stand-up is shown in Fig. 7. We use GPyTorch [57] to solve (6). For comparison, we provide a pseudo-random baseline based on space-filling Sobol sampling. The performance improvement over the episodes for five random seeds is plotted in Fig. 8. Even though, pseudo random sampling finds acceptable controllers eventually, BO has the better overall performance or requires less experiments with less failures.

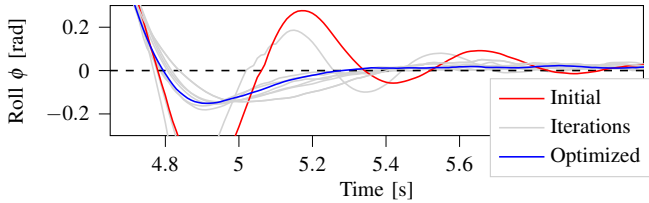


Fig. 7: State evolution for a hand-tuned controller (red), several episodes of BO (gray), and optimized controller (blue). The task is stabilizing after roll stand-up.

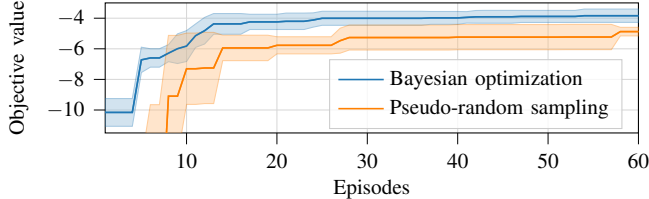


Fig. 8: Performance of the best controller found by BO (blue) for a given number of trials (episodes) compared to a pseudo-random baseline (orange). Intervals are the standard deviation over five random seeds.

B. Fast Neural Network Approximate MPC

Despite great engineering efforts, nonlinear solvers still struggle to solve MPC optimization problems in real-time on embedded CPUs. Instead, we use imitation learning to find an explicit mapping from states to actions in the form of a neural network that approximates the MPC described in Section IV-D. The approximate MPC is several orders of magnitude faster (onboard inference in less than 300 μ s) compared to solving the optimization problem (5), which takes several hundred milliseconds on a desktop CPU. It thus allows a sophisticated nonlinear MPC with convoluted system dynamics, fine discretization, and a long prediction horizon to run onboard the robot. With this, we achieve – for the first time – articulated driving following high level yaw and velocity setpoints, e.g., provided by keyboard.

We imitate the optimal solution to (5) by first sampling a large dataset of random states x and optimal solutions $u^*(x)$ containing 3.5 million points. We use a multi-layer perceptron with 4 layers, 100 neurons per layer, and a mixture of tangent hyperbolic and rectified linear activations as function approximator, which is trained in Jax. To achieve fast control, we implement inference in C++ using Eigen onboard the Mini Wheelbot. The final controller on the Mini Wheelbot hardware driving around based on keyboard heading and velocity commands is shown in Fig. 9 and the supplementary video. This is the first time that controlled driving along specified directions is achieved for a reaction wheel balancing unicycle of this kind.

VI. CONCLUSION

We introduce the new Mini Wheelbot, a balancing, reaction wheel unicycle robot designed as a robust, compact, and powerful testbed for learning-based control. We demonstrate the effectiveness of our platform in learning-based

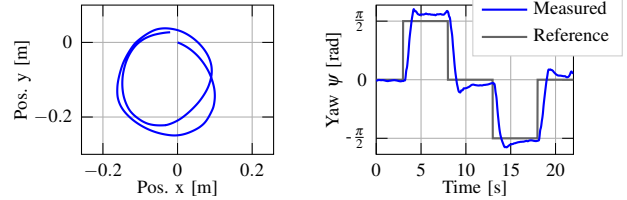


Fig. 9: Approximate MPC experiments: Driving around based on keyboard heading and velocity commands (left) and yaw reference step response (right). The controller runs onboard the Mini Wheelbot.

control tasks. First, we automatically tune the robot’s state-feedback controller using real-world experiments via BO. As BO requires repeated experiments, this demonstrates how the Mini Wheelbot’s automatic environment reset facilitates learning-based control. In a second illustrative application of learning-based control — imitation learning from an expert MPC — we show that sophisticated MPC schemes can be implemented without the burden of real-time optimization onboard the Mini Wheelbot. With this approximate MPC, we achieve yaw control and articulated driving for the first time in this class of robots. However, an in-depth theoretical analysis of this controller remains for future work.

During our experiments, we identified several open topics for future research. First, the estimator could be enhanced to handle singularities in the orientation representation and saturation in the gyroscope. Additionally, estimating contact could improve reliability of flip maneuvers and enable more acrobatic sequences with controlled contact switches. Second, with articulated driving now feasible, we plan to use a fleet of Mini Wheelbots to test future algorithmic advances in multi-robot coordination. Finally, the Mini Wheelbot has proven to be a robust testbed for learning through repeated experiments and automatic environment resets. As such, we envision benchmarking various learning algorithms, including reinforcement learning.

ACKNOWLEDGMENTS

We thank T. Beyer, P. Brunzema, D. Buchholz, R. Frohn, R. Geist, S. Giedyk, J. Menn, A. Mitri, and M. Ramirez.

REFERENCES

- [1] A. R. Geist, J. Fiene, N. Tashiro, Z. Jia, and S. Trimpe, “The Wheelbot: A jumping reaction wheel unicycle,” *IEEE Robotics and Automation Letters*, vol. 7, no. 4, pp. 9683–9690, 2022. (Secs. I, I, II, II-B, III-A, IV, 2, IV-C, IV-E, and V-A)
- [2] M. Hofer, M. Muehlebach, and R. D’Andrea, “The one-wheel Cubli: A 3d inverted pendulum that can balance with a single reaction wheel,” *Mechatronics*, vol. 91, p. 102965, 2023. (Secs. I, II, and II-B)

- [3] A. Carron, S. Bodmer, L. Vogel, R. Zurbrüggen, D. Helm, R. Rickenbach, S. Muntwiler, J. Sieber, and M. N. Zeilinger, "Chronos and CRS: Design of a miniature car-like robot and a software framework for single and multi-agent robotics and control," in *2023 IEEE International Conference on Robotics and Automation (ICRA)*. IEEE, 2023, pp. 1371–1378. (Secs. I, II, and II-A)
- [4] S. Bodmer, L. Vogel, S. Muntwiler, A. Hansson, T. Bodewig, J. Wahlen, M. N. Zeilinger, and A. Carron, "Optimization-based system identification and moving horizon estimation using low-cost sensors for a miniature car-like robot," *arXiv preprint arXiv:2404.08362*, 2024. (Secs. I, II, II-A, and IV-B)
- [5] M. O'Kelly, H. Zheng, D. Karthik, and R. Mangharam, "F1tenth: An open-source evaluation environment for continuous control and reinforcement learning," *Proceedings of Machine Learning Research*, vol. 123, 2020. (Secs. I, II, and II-A)
- [6] D. Hanover, A. Loquercio, L. Bauersfeld, A. Romero, R. Penicka, Y. Song, G. Cioffi, E. Kaufmann, and D. Scaramuzza, "Autonomous drone racing: A survey," *IEEE Transactions on Robotics*, 2024. (Sec. I)
- [7] S. Kim, P. M. Wensing *et al.*, "Design of dynamic legged robots," *Foundations and Trends® in Robotics*, vol. 5, no. 2, pp. 117–190, 2017. (Sec. I)
- [8] F. Mondada, E. Franzi, and P. Ienne, "Mobile robot miniaturisation: A tool for investigation in control algorithms," in *Experimental Robotics III: The 3rd International Symposium, Kyoto, Japan, October 28–30, 1993*. Springer, 1994, pp. 501–513. (Secs. II and II-A)
- [9] D. Johnson, T. Stack, R. Fish, D. M. Flickinger, L. Stoller, R. Ricci, and J. Lepreau, "Mobile emulab: A robotic wireless and sensor network testbed," in *Proceedings IEEE INFOCOM 2006. 25TH IEEE International Conference on Computer Communications*. IEEE, 2006, pp. 1–12. (Secs. II and II-A)
- [10] F. Mondada, M. Bonani, X. Raemy, J. Pugh, C. Cianci, A. Klaptocz, S. Magnenat, J.-C. Zufferey, D. Floreano, and A. Martinoli, "The e-puck, a robot designed for education in engineering," in *Proceedings of the 9th conference on autonomous robot systems and competitions*, vol. 1, no. 1. IPCB: Instituto Politécnico de Castelo Branco, 2009, pp. 59–65. (Secs. II and II-A)
- [11] M. Rubenstein, B. Cimino, R. Nagpal, and J. Werfel, "Aerobot: An affordable one-robot-per-student system for early robotics education," in *2015 IEEE International Conference on Robotics and Automation (ICRA)*. IEEE, 2015, pp. 6107–6113. (Secs. II and II-A)
- [12] D. Pickem, M. Lee, and M. Egerstedt, "The gritsbot in its natural habitat—a multi-robot testbed," in *2015 IEEE International conference on robotics and automation (ICRA)*. IEEE, 2015, pp. 4062–4067. (Secs. II and II-A)
- [13] S. Wilson, R. Gamos, M. Sheely, M. Lin, K. Dover, R. Gevorkyan, M. Haberland, A. Bertozzi, and S. Berman, "Pheeno, a versatile swarm robotic research and education platform," *IEEE Robotics and Automation Letters*, vol. 1, no. 2, pp. 884–891, 2016. (Secs. II and II-A)
- [14] L. Paull, J. Tani, H. Ahn, J. Alonso-Mora, L. Carlone, M. Cap, Y. F. Chen, C. Choi, J. Dusek, Y. Fang *et al.*, "Duckietown: an open, inexpensive and flexible platform for autonomy education and research," in *2017 IEEE International Conference on Robotics and Automation (ICRA)*. IEEE, 2017, pp. 1497–1504. (Secs. II and II-A)
- [15] C. H. Hsieh, Y.-L. Chuang, Y. Huang, K. K. Leung, A. L. Bertozzi, and E. Frazzoli, "An economical micro-car testbed for validation of cooperative control strategies," in *2006 American Control Conference*. IEEE, 2006, pp. 6–pp. (Secs. II and II-A)
- [16] A. Liniger, A. Domahidi, and M. Morari, "Optimization-based autonomous racing of 1: 43 scale RC cars," *Optimal Control Applications and Methods*, vol. 36, no. 5, pp. 628–647, 2015. (Secs. II and II-A)
- [17] B. Goldfain, P. Drews, C. You, M. Barulic, O. Velev, P. Tsiotras, and J. M. Rehg, "Autorally: An open platform for aggressive autonomous driving," *IEEE Control Systems Magazine*, vol. 39, no. 1, pp. 26–55, 2019. (Secs. II and II-A)
- [18] J. M. Gonzales, *Planning and control of drift maneuvers with the Berkeley autonomous race car*. University of California, Berkeley, 2018. (Secs. II and II-A)
- [19] M. Gajamohan, M. Merz, I. Thommen, and R. D'Andrea, "The Cubli: A cube that can jump up and balance," in *2012 IEEE/RSJ International Conference on Intelligent Robots and Systems*. IEEE, 2012, pp. 3722–3727. (Secs. II, II-B, and IV)
- [20] J. Mayr, F. Spanlang, and H. Gatttringer, "Mechatronic design of a self-balancing three-dimensional inertia wheel pendulum," *Mechatronics*, vol. 30, pp. 1–10, 2015. (Secs. II and II-B)
- [21] M. Muehlebach and R. D'Andrea, "Nonlinear analysis and control of a reaction wheel-based 3-d inverted pendulum," *IEEE Transactions on Control Systems Technology*, vol. 25, no. 1, pp. 235–246, 2016. (Secs. II, II-B, and IV)
- [22] V. Klemm, A. Morra, C. Salzmann, F. Tschopp, K. Bodie, L. Gulich, N. Küng, D. Mannhart, C. Pfister, M. Vierneisel *et al.*, "Ascento: A two-wheeled jumping robot," in *2019 International Conference on Robotics and Automation (ICRA)*. IEEE, 2019, pp. 7515–7521. (Secs. II and II-B)
- [23] U. Nagarajan, G. Kantor, and R. Hollis, "The Ballbot: An omnidirectional balancing mobile robot," *The International Journal of Robotics Research*, vol. 33, no. 6, pp. 917–930, 2014. (Secs. II and II-B)
- [24] D. Pickem, P. Glotfelter, L. Wang, M. Mote, A. Ames, E. Feron, and M. Egerstedt, "The robotarium: A remotely accessible swarm robotics research testbed," in *2017 IEEE International Conference on Robotics and Automation (ICRA)*. IEEE, 2017, pp. 1699–1706. (Sec. II-A)
- [25] A. Schwab, L.-M. Reichelt, P. Welz, and J. Lunze, "Experimental evaluation of an adaptive cruise control and cooperative merging concept," in *2020 IEEE Conference on Control Technology and Applications (CCTA)*. IEEE, 2020, pp. 318–325. (Sec. II-A)
- [26] S. Trimpe and R. D'Andrea, "The balancing cube: A dynamic sculpture as test bed for distributed estimation and control," *IEEE Control Systems Magazine*, vol. 32, no. 6, pp. 48–75, 2012. (Secs. II-B and IV)
- [27] A. Schoonwinkel, *Design and test of a computer-stabilized unicycle*. Stanford University, 1988. (Sec. II-B)
- [28] D. W. Vos and A. H. Von Flotow, "Dynamics and nonlinear adaptive control of an autonomous unicycle: Theory and experiment," in *29th IEEE Conference on Decision and Control*. IEEE, 1990, pp. 182–187. (Sec. II-B)
- [29] J.-X. Xu, A. Al Mamun, and Y. Daud, "Pendulum-balanced autonomous unicycle: Conceptual design and dynamics model," in *2011 IEEE 5th international conference on robotics, automation and mechatronics (ram)*. IEEE, 2011, pp. 51–56. (Sec. II-B)
- [30] Y. Daud, A. Al Mamun, and J.-X. Xu, "Dynamic modeling and characteristics analysis of lateral-pendulum unicycle robot," *Robotica*, vol. 35, no. 3, pp. 537–568, 2017. (Secs. II-B and IV-A)
- [31] J. Lee, S. Han, and J. Lee, "Decoupled dynamic control for pitch and roll axes of the unicycle robot," *IEEE Transactions on Industrial Electronics*, vol. 60, no. 9, pp. 3814–3822, 2012. (Sec. II-B)
- [32] L. Jae-Oh, H. In-Woo, and L. Jang-Myung, "Fuzzy sliding mode control of unicycle robot," in *2011 8th international conference on ubiquitous robots and ambient intelligence (urai)*. IEEE, 2011, pp. 521–524. (Sec. II-B)
- [33] Y. Li, J.-O. Lee, and J. Lee, "Attitude control of the unicycle robot using fuzzy-sliding mode control," in *Intelligent Robotics and Applications: 5th International Conference, ICIRA 2012, Montreal, QC, Canada, October 3-5, 2012, Proceedings, Part III 5*. Springer, 2012, pp. 62–72. (Sec. II-B)
- [34] M. A. Rosyidi, E. H. Binugroho, S. E. R. Charel, R. S. Dewanto, and D. Pramadihanto, "Speed and balancing control for unicycle robot," in *2016 International Electronics Symposium (IES)*. IEEE, 2016, pp. 19–24. (Sec. II-B)
- [35] G. P. Neves and B. A. Angélico, "A discrete lqr applied to a self-balancing reaction wheel unicycle: Modeling, construction and control," in *2021 American control conference (ACC)*. IEEE, 2021, pp. 777–782. (Sec. II-B)
- [36] Y. Rizal, C.-T. Ke, and M.-T. Ho, "Point-to-point motion control of a unicycle robot: Design, implementation, and validation," in *2015 IEEE International Conference on Robotics and Automation (ICRA)*. IEEE, 2015, pp. 4379–4384. (Sec. II-B)
- [37] H. Jin, J. Hwang, and J. Lee, "A balancing control strategy for a one-wheel pendulum robot based on dynamic model decomposition: Simulations and experiments," *IEEE/ASME Transactions on Mechatronics*, vol. 16, no. 4, pp. 763–768, 2010. (Sec. II-B)
- [38] R. Lehmann, Se-Bi, N. Hauser, and C. Lutz, "µMotor: A motor controller for BLDC and DC motors up to 250W." [Online]. Available: <https://github.com/roboterclubaachen/micro-motor> (Sec. III-B)
- [39] M. Piccoli and M. Yim, "Anticogging: Torque ripple suppression, modeling, and parameter selection," *The international journal of robotics research*, vol. 35, no. 1-3, pp. 148–160, 2016. (Sec. III-B)
- [40] S. Trimpe and R. D'Andrea, "Accelerometer-based tilt estimation of a rigid body with only rotational degrees of freedom," in *2010 IEEE International Conference on Robotics and Automation*. IEEE, 2010, pp. 2630–2636. (Sec. IV)

- [41] J. Frey, J. De Schutter, and M. Diehl, “Fast integrators with sensitivity propagation for use in CasADi,” in *2023 European Control Conference (ECC)*. IEEE, 2023. (Sec. IV-A)
- [42] H. G. Bock, “Recent advances in parameter identification techniques for ODE,” in *Numerical Treatment of Inverse Problems in Differential and Integral Equations: Proceedings of an International Workshop, Heidelberg, Fed. Rep. of Germany, August 30—September 3, 1982*. Springer, 1983, pp. 95–121. (Sec. IV-B)
- [43] J. Valluru, P. Lakhmani, S. C. Patwardhan, and L. T. Biegler, “Development of moving window state and parameter estimators under maximum likelihood and bayesian frameworks,” *Journal of Process Control*, vol. 60, pp. 48–67, 2017. (Sec. IV-B)
- [44] L. Simpson, A. Ghezzi, J. Asprión, and M. Diehl, “An efficient method for the joint estimation of system parameters and noise covariances for linear time-variant systems,” in *2023 62nd IEEE Conference on Decision and Control (CDC)*. IEEE, 2023, pp. 4524–4529. (Sec. IV-B)
- [45] J. A. Andersson, J. Gillis, G. Horn, J. B. Rawlings, and M. Diehl, “Casadi: a software framework for nonlinear optimization and optimal control,” *Mathematical Programming Computation*, vol. 11, pp. 1–36, 2019. (Secs. IV-B and IV-D)
- [46] A. Wächter and L. T. Biegler, “On the implementation of an interior-point filter line-search algorithm for large-scale nonlinear programming,” *Mathematical programming*, vol. 106, pp. 25–57, 2006. (Secs. IV-B and IV-D)
- [47] J. B. Rawlings, D. Q. Mayne, M. Diehl *et al.*, *Model predictive control: Theory, computation, and design*. Nob Hill Publishing Madison, WI, 2017, vol. 2. (Sec. IV-D)
- [48] K. Chatzilygeroudis, V. Vassiliades, F. Stulp, S. Calinon, and J.-B. Mouret, “A survey on policy search algorithms for learning robot controllers in a handful of trials,” *IEEE Transactions on Robotics*, vol. 36, no. 2, pp. 328–347, 2019. (Secs. V and V-A)
- [49] J. A. Paulson, F. Sorourifar, and A. Mesbah, “A tutorial on derivative-free policy learning methods for interpretable controller representations,” in *2023 American Control Conference (ACC)*, 2023, pp. 1295–1306. (Secs. V and V-A)
- [50] A. Marco, P. Hennig, J. Bohg, S. Schaal, and S. Trimpe, “Automatic LQR tuning based on Gaussian process global optimization,” in *2016 IEEE international conference on robotics and automation (ICRA)*. IEEE, 2016, pp. 270–277. (Secs. V and V-A)
- [51] R. Calandra, A. Seyfarth, J. Peters, and M. P. Deisenroth, “Bayesian optimization for learning gaits under uncertainty: An experimental comparison on a dynamic bipedal walker,” *Annals of Mathematics and Artificial Intelligence*, vol. 76, pp. 5–23, 2016. (Secs. V and V-A)
- [52] F. Berkenkamp, A. P. Schoellig, and A. Krause, “Safe controller optimization for quadrotors with gaussian processes,” in *2016 IEEE international conference on robotics and automation (ICRA)*. IEEE, 2016, pp. 491–496. (Secs. V and V-A)
- [53] C. Gonzalez, H. Asadi, L. Kooijman, and C. P. Lim, “Neural networks for fast optimisation in model predictive control: a review,” *arXiv preprint arXiv:2309.02668*, 2023. (Sec. V)
- [54] J. Carius, F. Farshidian, and M. Hutter, “MPC-Net: A first principles guided policy search,” *IEEE Robotics and Automation Letters*, vol. 5, no. 2, pp. 2897–2904, 2020. (Sec. V)
- [55] J. Nubert, J. Köhler, V. Berenz, F. Allgöwer, and S. Trimpe, “Safe and fast tracking on a robot manipulator: Robust MPC and neural network control,” *IEEE Robotics and Automation Letters*, vol. 5, no. 2, pp. 3050–3057, 2020. (Sec. V)
- [56] H. Hose, A. Gräfe, and S. Trimpe, “Parameter-adaptive approximate MPC: Tuning neural-network controllers without retraining,” in *Proceedings of the 6th Annual Learning for Dynamics and Control Conference*, ser. Proceedings of Machine Learning Research, A. Abate, M. Cannon, K. Margellos, and A. Papachristodoulou, Eds., vol. 242. PMLR, 15–17 Jul 2024, pp. 349–360. (Sec. V)
- [57] J. Gardner, G. Pleiss, K. Q. Weinberger, D. Bindel, and A. G. Wilson, “Gpytorch: Blackbox matrix-matrix gaussian process inference with GPU acceleration,” *Advances in neural information processing systems*, vol. 31, 2018. (Sec. V-A)